Supporting information for: Development and Validation of AMBER-FB15-compatible Force Field Parameters for Phosphorylated Amino Acids

John P. Stoppelman,[†] Tracey T. Ng,[‡] Paul S. Nerenberg,[*,‡,¶] and Lee-Ping Wang[*,§]

[†]*School of Chemistry and Biochemistry, Georgia Institute of Technology, Atlanta, GA 30332-0400, United States*

[‡]*Department of Physics & Astronomy, California State University, Los Angeles, CA 90032, United States*

[¶]*Department of Biological Sciences, California State University, Los Angeles, CA 90032, United States*

[§]*Department of Chemistry, University of California, Davis, CA 95616, United States*

E-mail: pnerenb@calstatela.edu; leeping@ucdavis.edu

1 Optimized Force Field Parameters

1.1 Residues and Parameter Types

The tables below list the atom names, atom types and element making up each residue. The * indicates the newly introduced β carbon atom types (as well as γ carbon types in the case of phosphorylated threonine) which were made for each residue.

Table S1: List of atom types for monoanionic phosphorylated serine (S1P)

Atom Name	Atom Type	Element
HH31	HC	H
CH3	CT	C
HH32	HC	H
HH33	HC	H
C	C	C
O	O	O
N	N	N
H	H	H
CA	CT	C
HA	H1	H
CB	bs*	C
HB1	H1	H
HB2	H1	H
OG	OR	O
P	P	P
O1P	OQ	O
O2P	OP	O
O3P	OP	O
H1P	HO	H
C	C	C
O	O	O
N	N	N
H	H	H
CH3	CT	C
HH31	H1	H
HH32	H1	H
HH33	H1	H

Table S2: List of atom types for dianionic phosphorylated serine (SEP)

Atom Name	Atom Type	Element
HH31	HC	H
CH3	CT	C
HH32	HC	H
HH33	HC	H
C	C	C
O	O	O
N	N	N
H	H	H
CA	CT	C
HA	H1	H
CB	BS*	C
HB1	H1	H
HB2	H1	H
OG	OZ	O
P	P	P
O1P	OX	O
O2P	OX	O
O3P	OX	O
C	C	C
O	O	O
N	N	N
H	H	H
CH3	CT	C
HH31	H1	H
HH32	H1	H
HH33	H1	H

Table S3: List of atom types for monoanionic phosphorylated threonine (T1P)

Atom Name	Atom Type	Element
HH31	HC	H
CH3	CT	C
HH32	HC	H
HH33	HC	H
C	C	C
O	O	O
N	N	N
H	H	H
CA	CT	C
HA	H1	H
CB	bt*	C
HB	H1	H
CG2	gt*	C
HG21	HC	H
HG22	HC	H
HG23	HC	H
OG1	OR	O
P	P	P
O1P	OQ	O
O2P	OP	O
O3P	OP	O
H1P	HO	H
C	C	C
O	O	O
N	N	N
H	H	H
CH3	CT	C
HH31	H1	H
HH32	H1	H
HH33	H1	H

Table S4: List of atom types for dianionic phosphorylated threonine (TPO)

Atom Name	Atom Type	Element
HH31	HC	H
CH3	CT	C
HH32	HC	H
HH33	HC	H
C	C	C
O	O	O
N	N	N
H	H	H
CA	CT	C
HA	H1	H
CB	BT*	C
HB	H1	H
CG2	GT*	C
HG21	HC	H
HG22	HC	H
HG23	HC	H
OG1	OZ	O
P	P	P
O1P	OX	O
O2P	OX	O
O3P	OX	O
C	C	C
O	O	O
N	N	N
H	H	H
CH3	CT	C
HH31	H1	H
HH32	H1	H
HH33	H1	H

Table S5: List of atom types for monoanionic phosphorylated tyrosine (Y1P)

Atom Name	Atom Type	Element
HH31	HC	H
CH3	CT	C
HH32	HC	H
HH33	HC	H
C	C	C
O	O	O
N	N	N
H	H	H
CA	CT	C
HA	H1	H
CB	by*	C
HB1	HC	H
HB2	HC	H
CG	CA	C
CD1	CA	C
HD1	HA	H
CE1	CA	C
HE1	HA	H
CZ	C	C
CE2	CA	C
HE2	HA	H
CD2	CA	C
HD2	HA	H
OG	OR	O
P	P	P
O1P	OQ	O
O2P	OP	O
O3P	OP	O
H1P	HO	H
C	C	C
O	O	O
N	N	N
H	H	H
CH3	CT	C
HH31	H1	H
HH32	H1	H
HH33	H1	H

Table S6: List of atom types for dianionic phosphorylated tyrosine (PTR)

Atom Name	Atom Type	Element
HH31	HC	H
CH3	CT	C
HH32	HC	H
HH33	HC	H
C	C	C
O	O	O
N	N	N
H	H	H
CA	CT	C
HA	H1	H
CB	BY*	C
HB1	HC	H
HB2	HC	H
CG	CA	C
CD1	CA	C
HD1	HA	H
CE1	CA	C
HE1	HA	H
CZ	C	C
CE2	CA	C
HE2	HA	H
CD2	CA	C
HD2	HA	H
OH	OV	O
P	P	P
O1P	OT	O
O2P	OT	O
O3P	OT	O
C	C	C
O	O	O
N	N	N
H	H	H
CH3	CT	C
HH31	H1	H
HH32	H1	H
HH33	H1	H

1.2 Initial Parameter Changes for Dianionic Residues

As noted in the main text, we altered the AMBER ff99SB equilibrium bond length parameters for the bridging oxygen-phosphorous bonds in the dianionic residues (OZ-P in SEP and TPO/OV-P in PTR).[S1] Both of these parameters are 0.161 nm in ff99SB. Upon performing geometry optimizations of dianionic methyl phosphate and phenyl phosphate (analogues for SEP/TPO and PTR, respectively) at the MP2/aug-cc-pVTZ level of theory, we find that the bond lengths are ∼0.18 nm for the bridging oxygen-phosphorous bond in methyl phosphate and ∼0.19 nm in phenyl phosphate. Additionally, we find that the average bond length from our grids of geometry optimizations for OZ-P in SEP/TPO is ∼0.18 nm, while the average bond length for OV-P in PTR is ∼0.195 nm. Based on these results, we increased the initial bond length parameter value for OZ-P to 0.18 nm and the initial parameter value for OV-P to 0.19 nm in order to provide a better initial guess for ForceBalance.

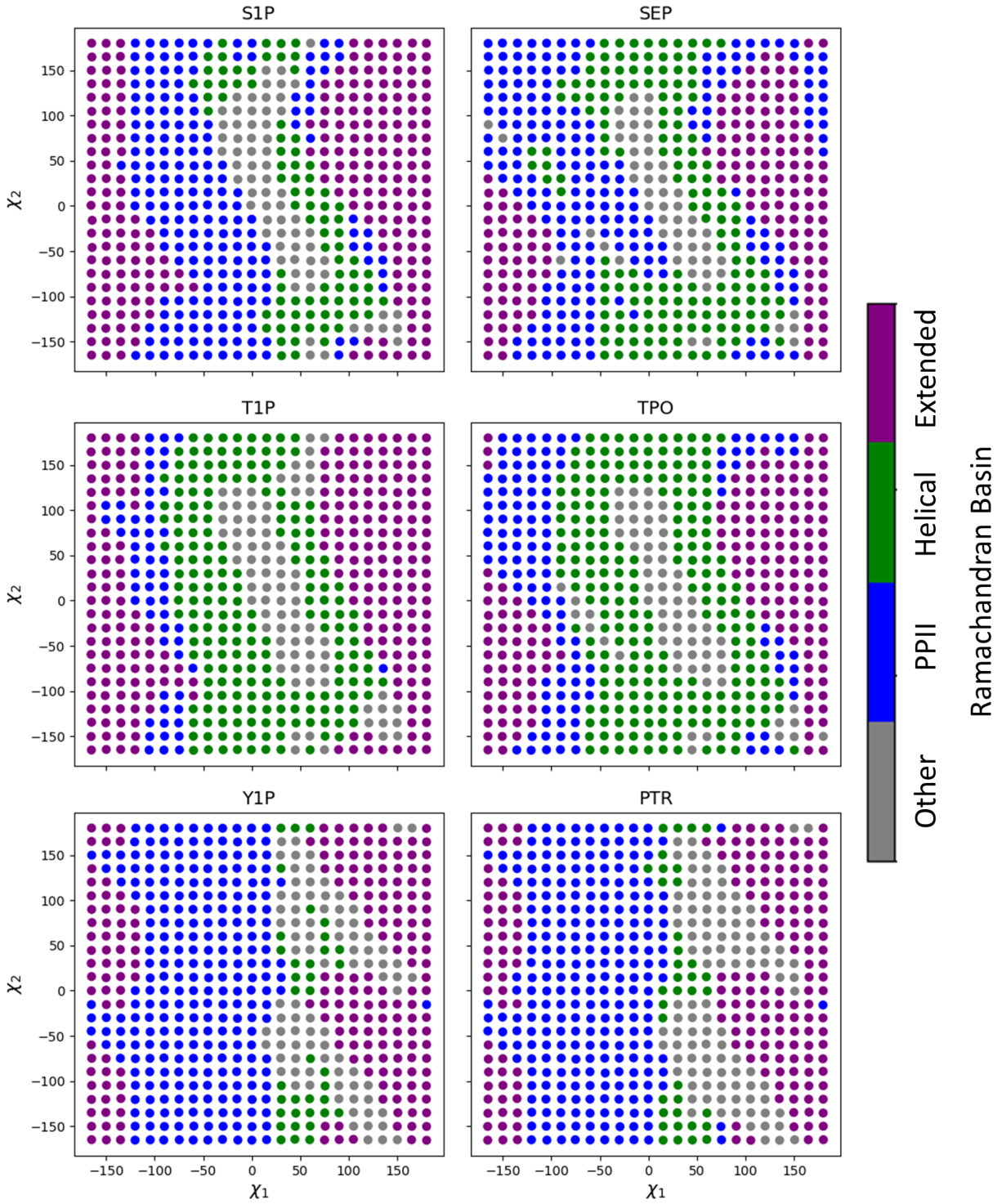

Figure S1: The Ramachandran basin of the optimized ϕ/ψ dihedral angles corresponding to each χ_1/χ_2 grid point for the χ_1/χ_2 dihedral scans. Basin definitions follow the definitions of Vymětal *et al.*[S2]

1.3 Optimized Bond Parameters

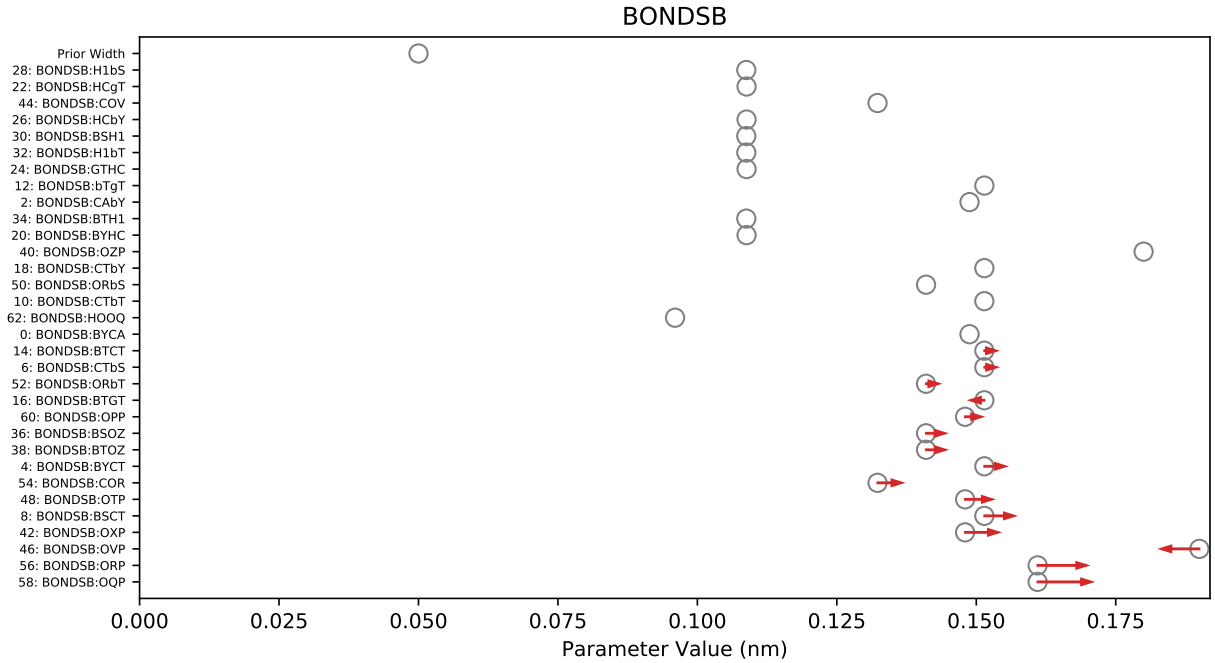

Figure S2: Parameter changes for the equilibrium bond lengths.

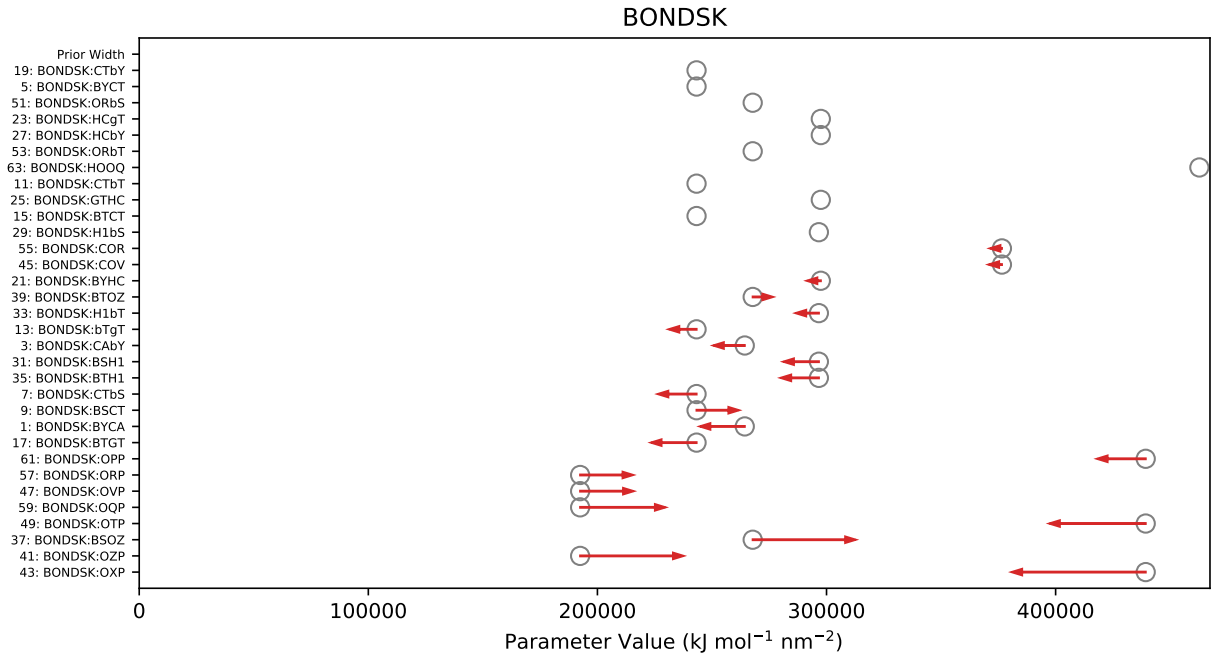

Figure S3: Parameter changes for the bond force constants.

1.4 Optimized Angle Parameters

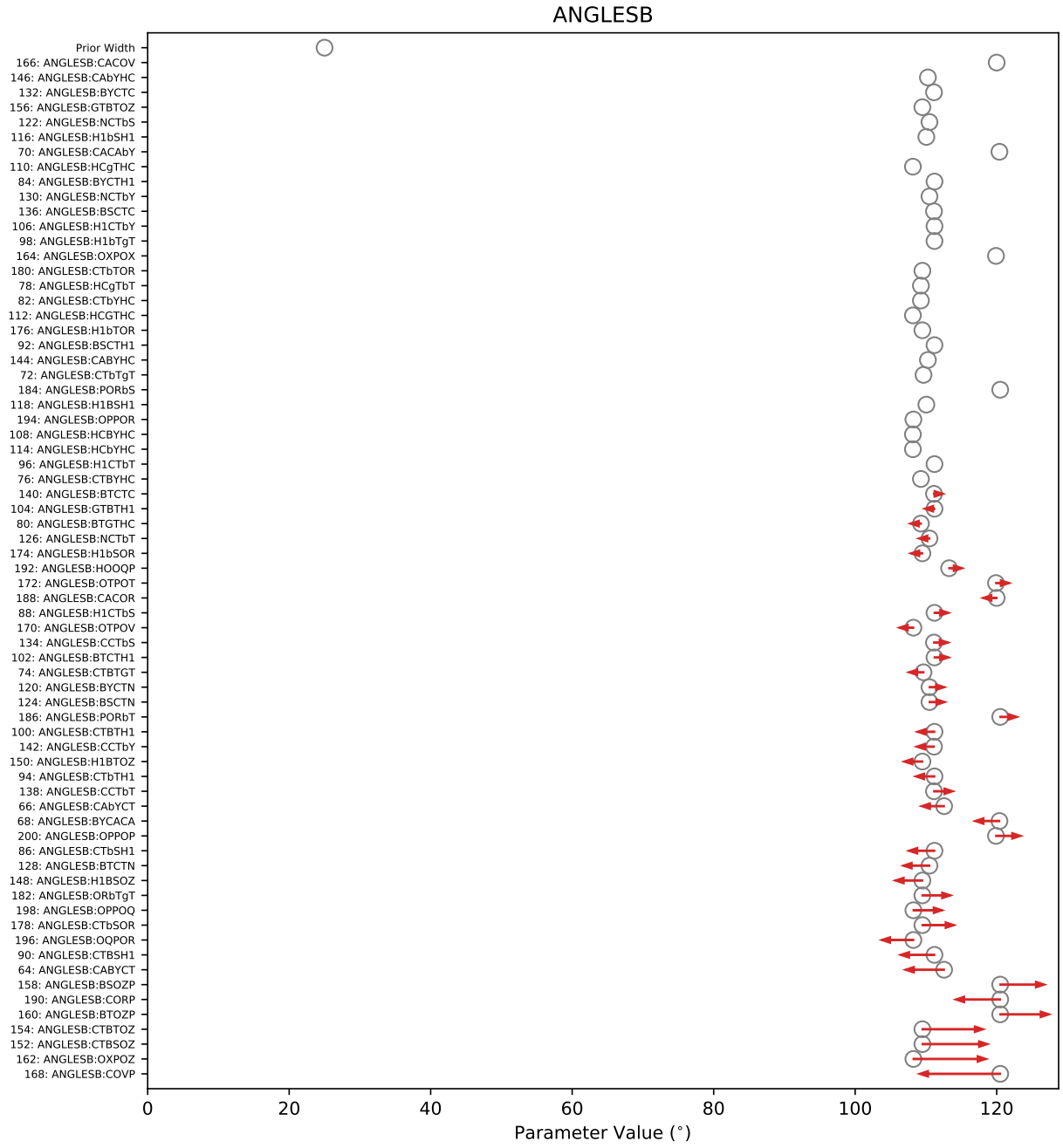

Figure S4: Parameter changes for the equilibrium angle values.

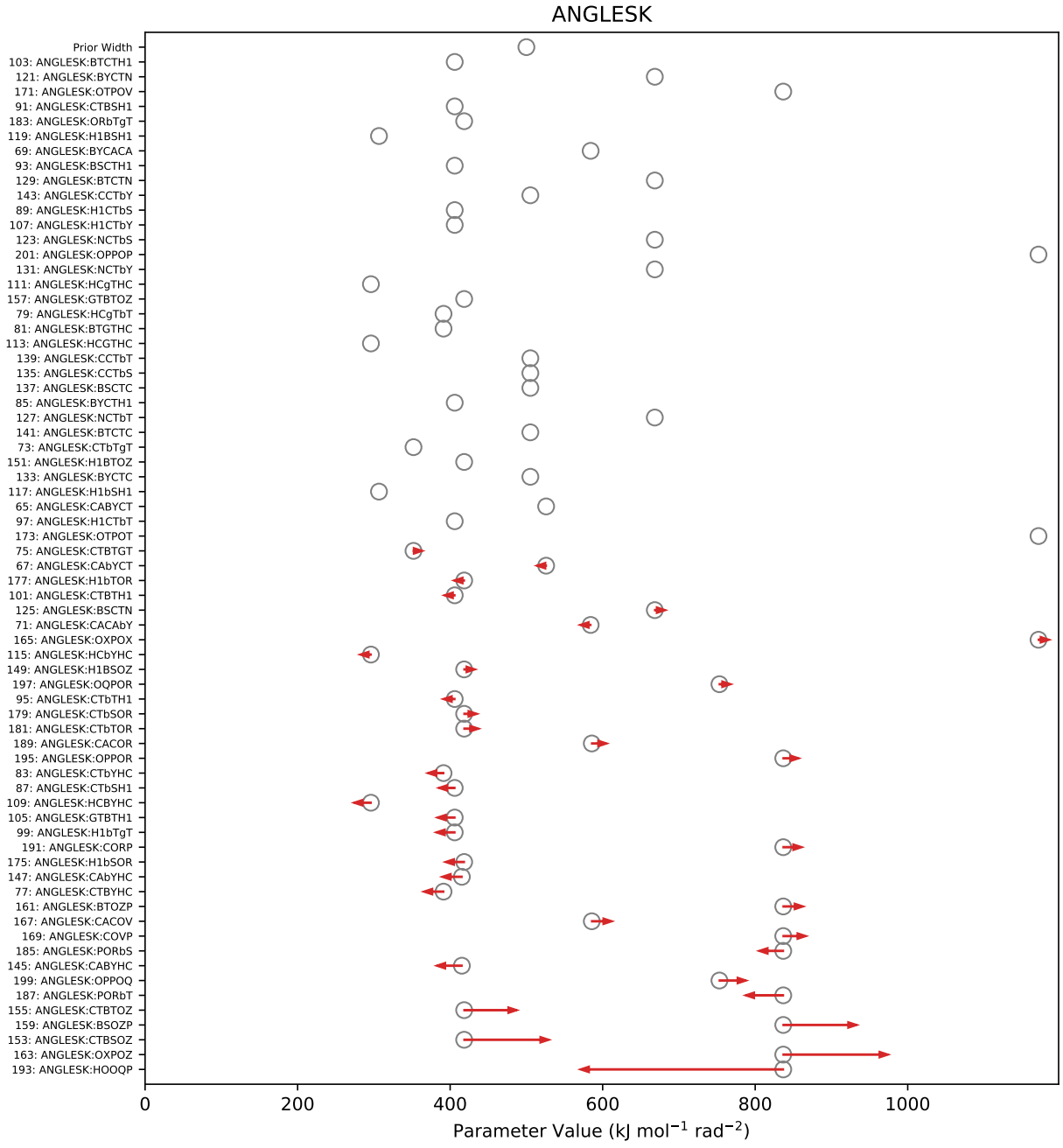

Figure S5: Parameter changes for the angle force constants.

1.5 Optimized Proper Dihedral Parameters

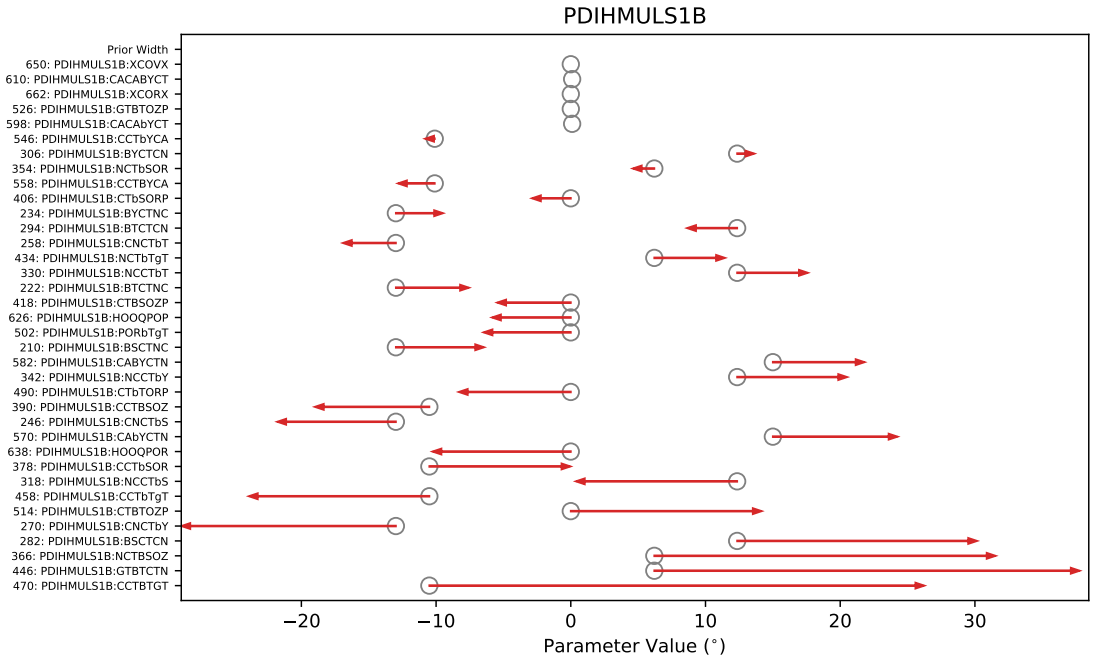

Figure S6: Parameter changes for the proper dihedral angle values (multiplicity 1).

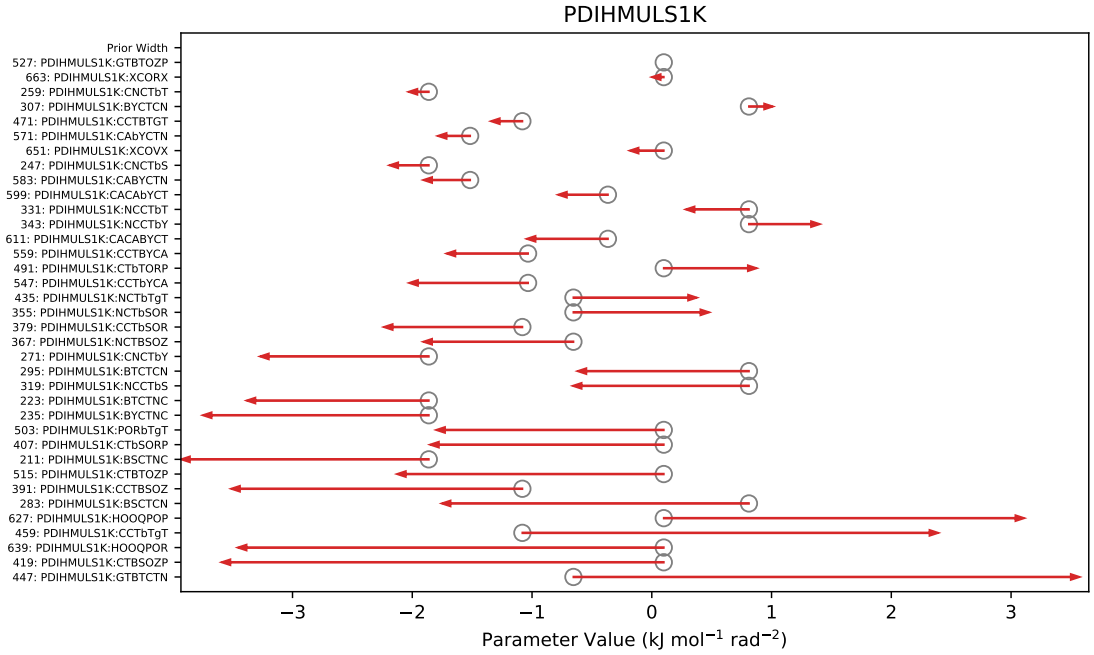

Figure S7: Parameter changes for the proper dihedral force constants (multiplicity 1).

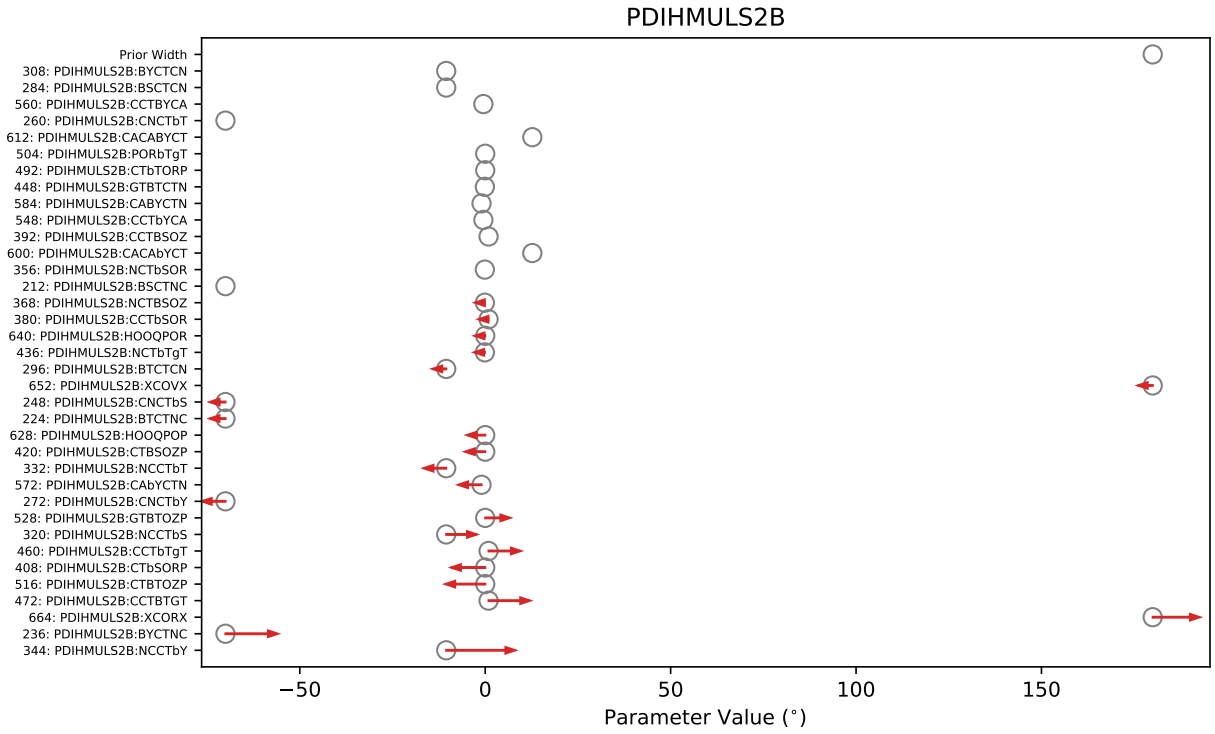

Figure S8: Parameter changes for the proper dihedral angle values (multiplicity 2).

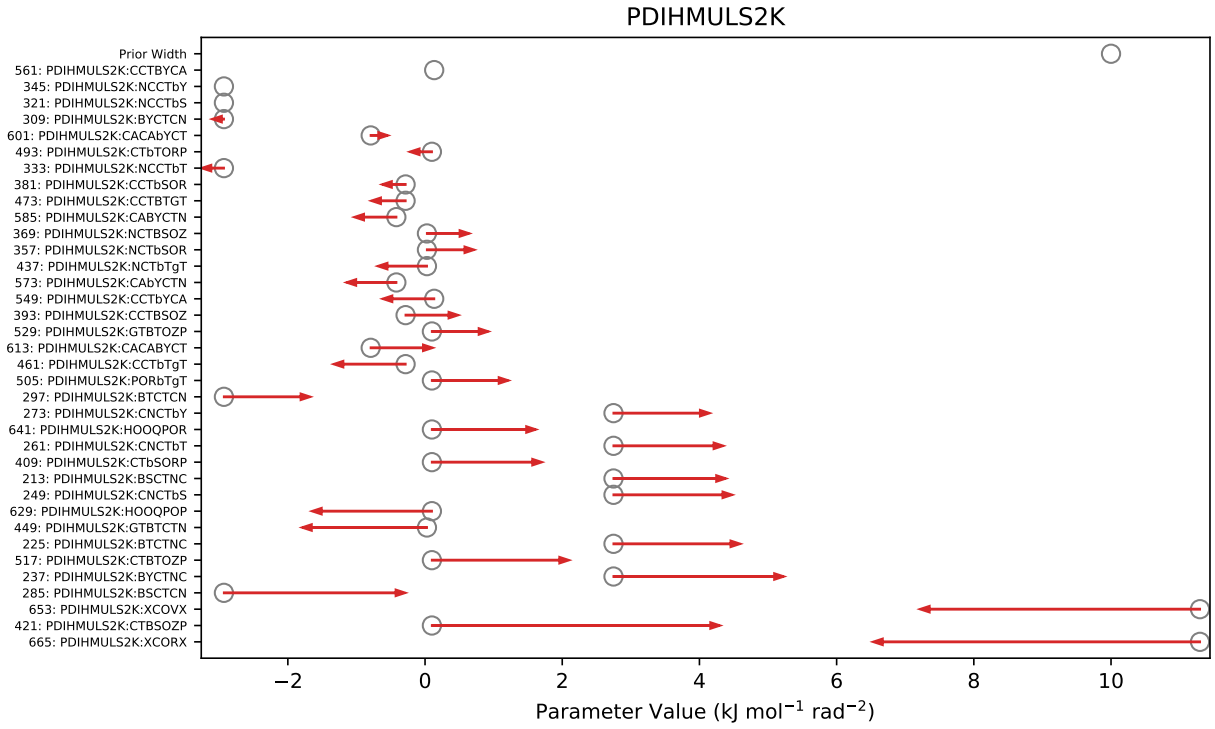

Figure S9: Parameter changes for the proper dihedral force constants (multiplicity 2).

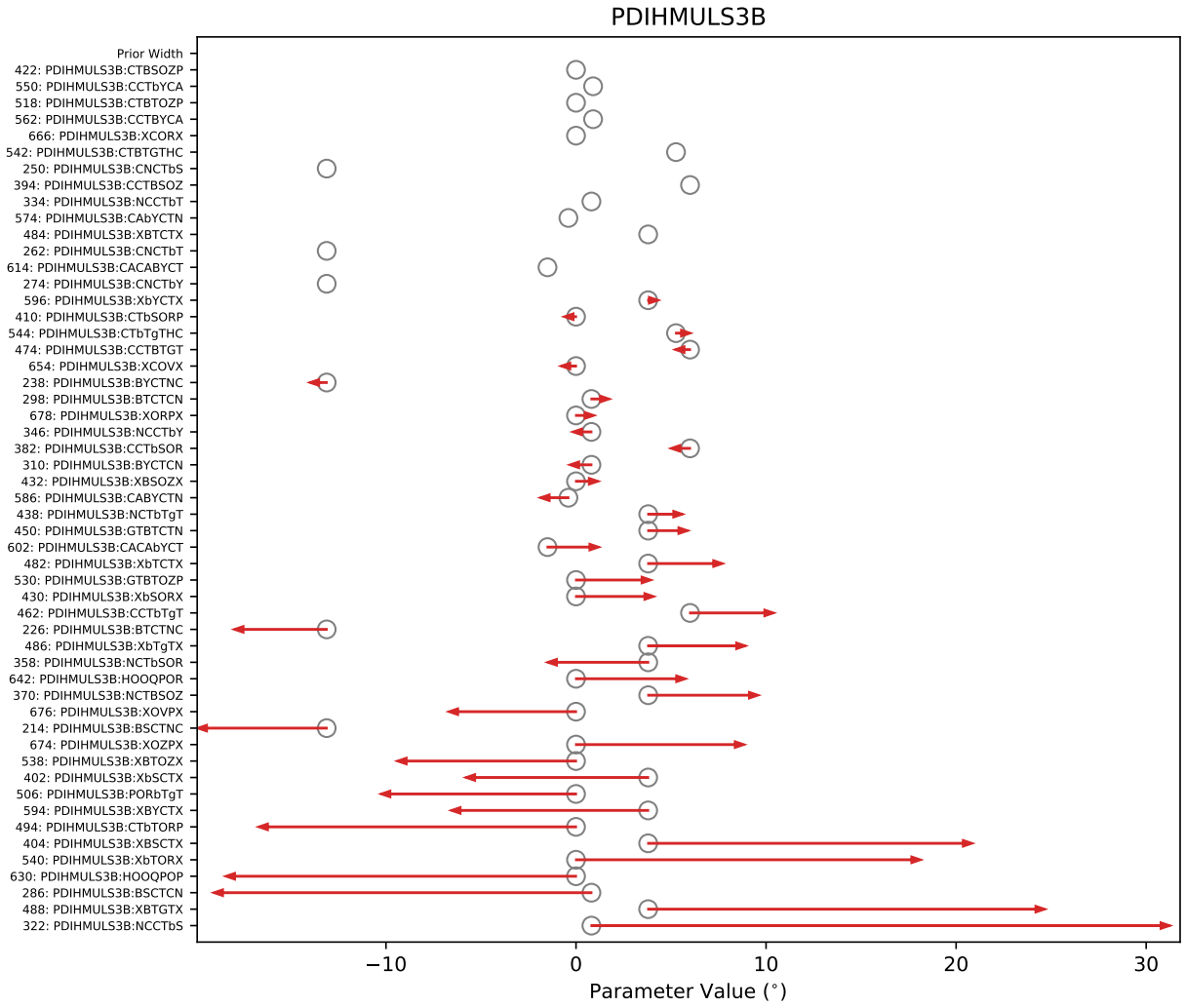

Figure S10: Parameter changes for the proper dihedral angle values (multiplicity 3).

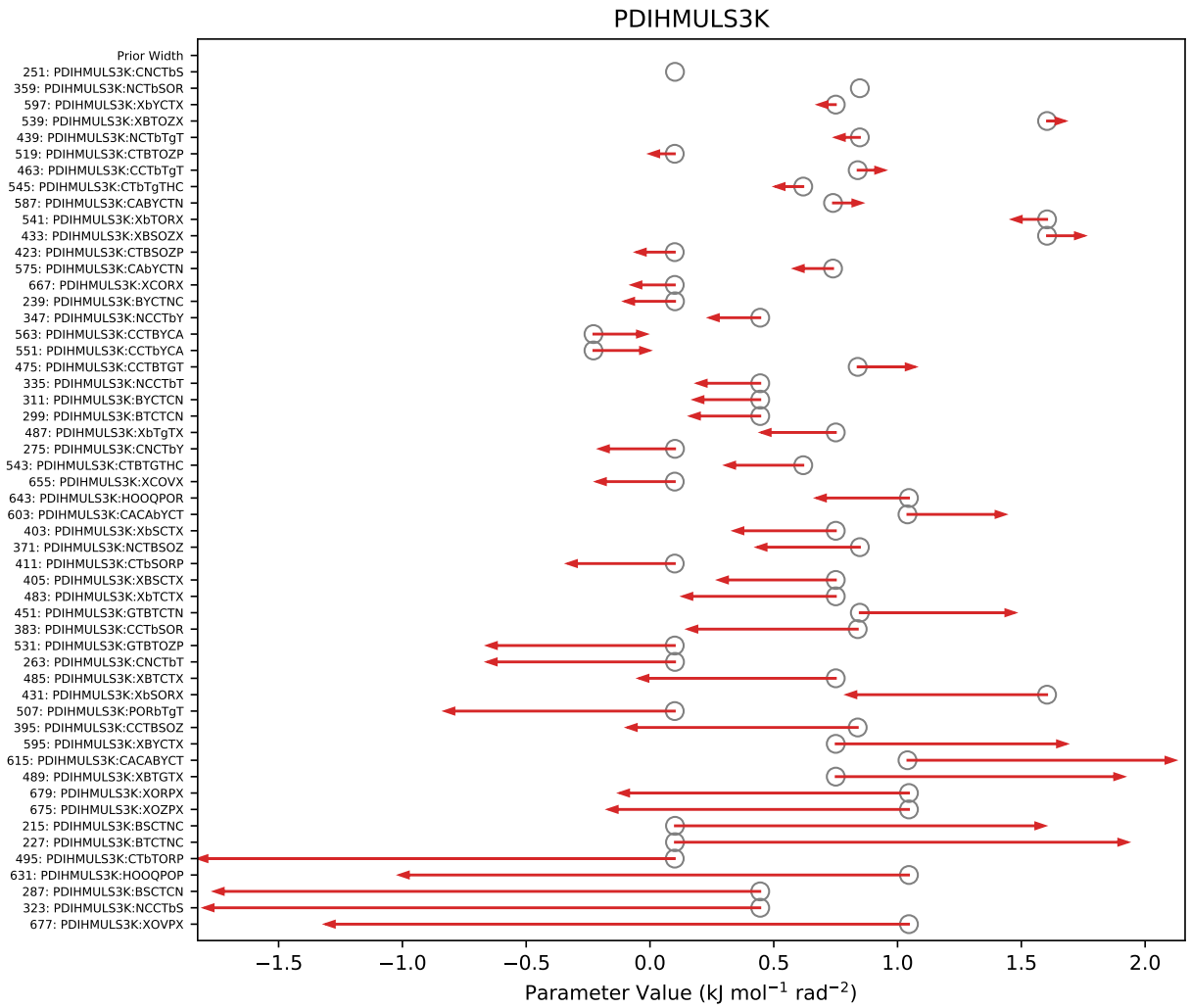

Figure S11: Parameter changes for the proper dihedral force constants (multiplicity 3).

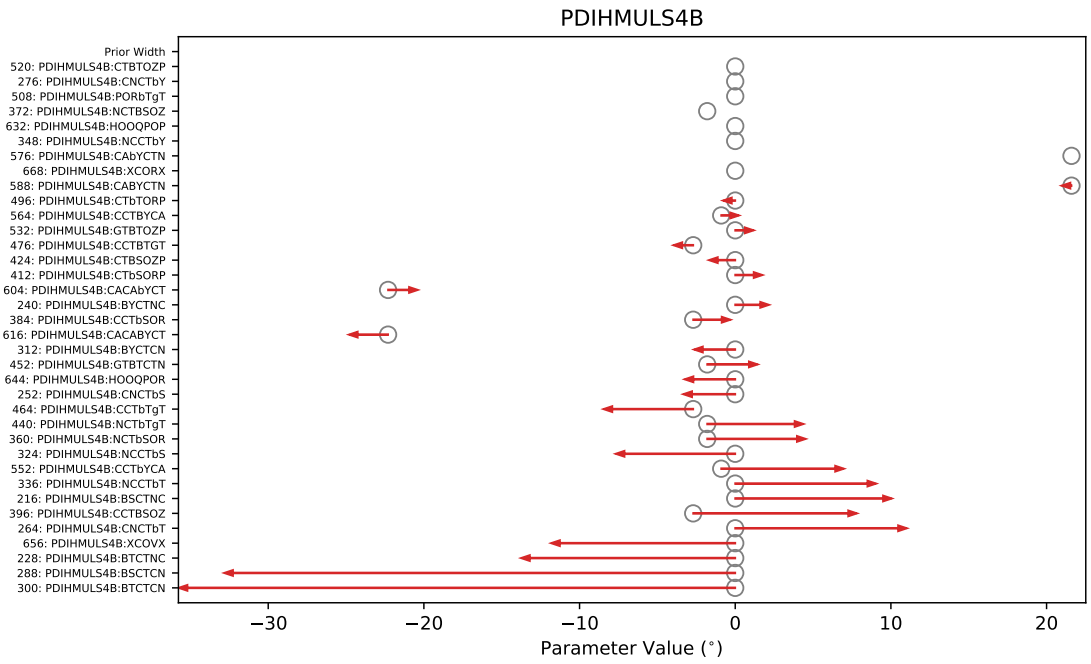

Figure S12: Parameter changes for the proper dihedral angle values (multiplicity 4).

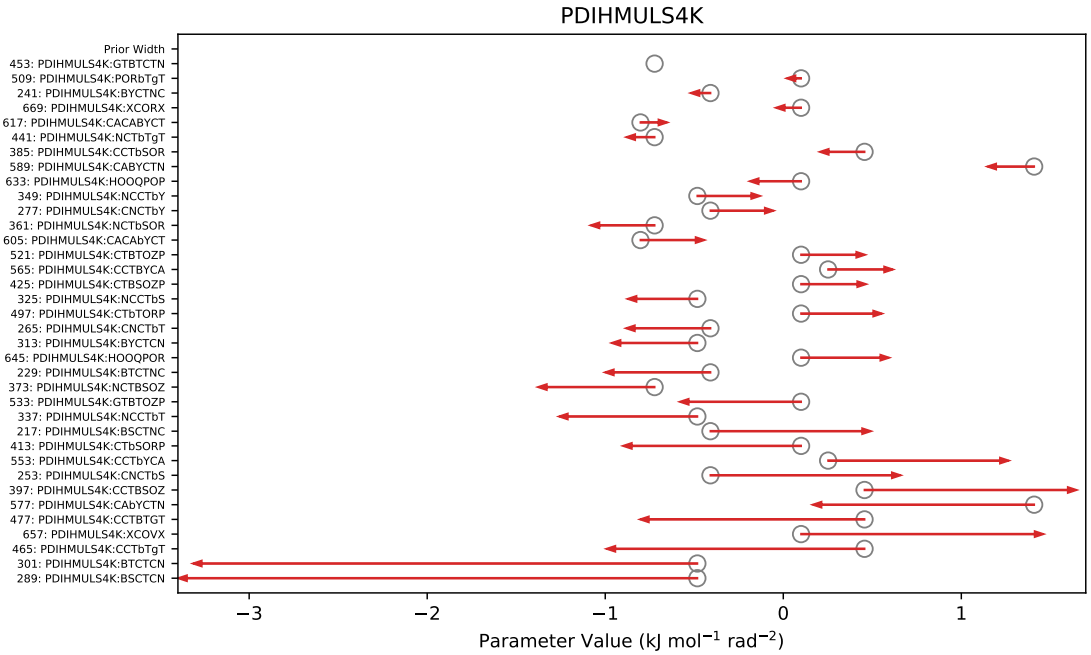

Figure S13: Parameter changes for the proper dihedral angle force constants (multiplicity 4).

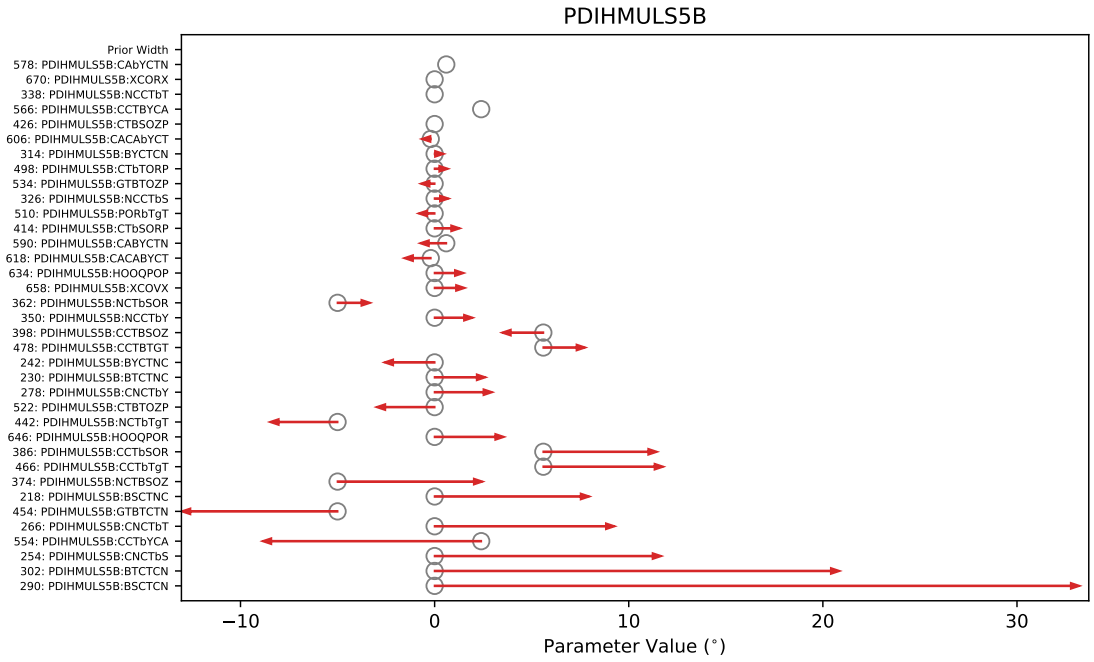

Figure S14: Parameter changes for the proper dihedral angle values (multiplicity 5).

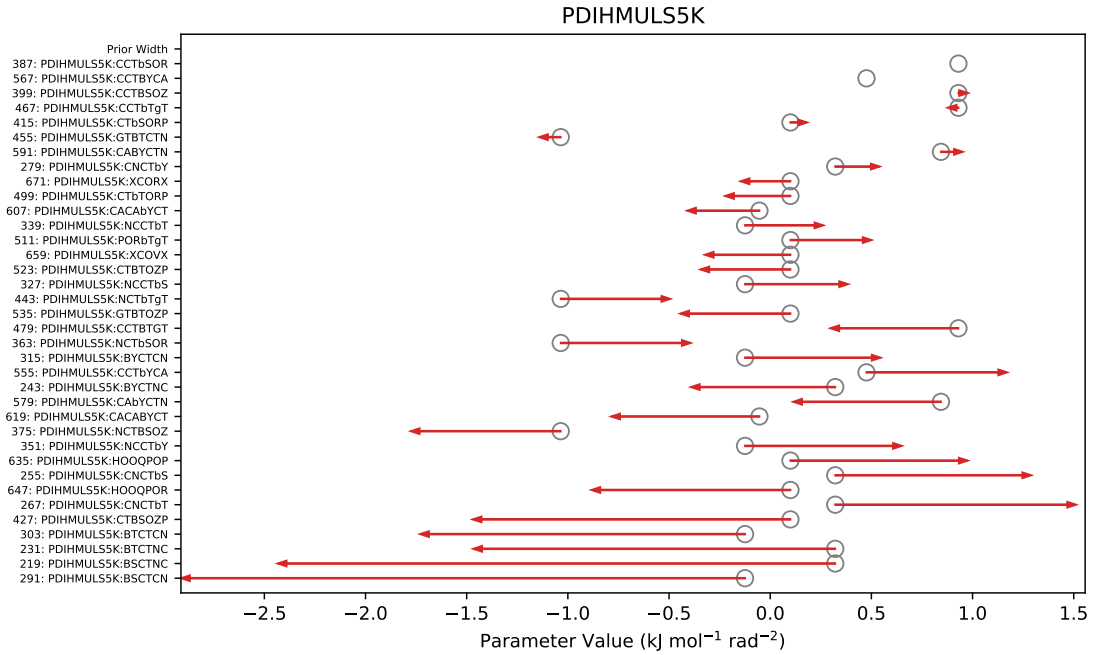

Figure S15: Parameter changes for the proper dihedral angle force constants (multiplicity 5).

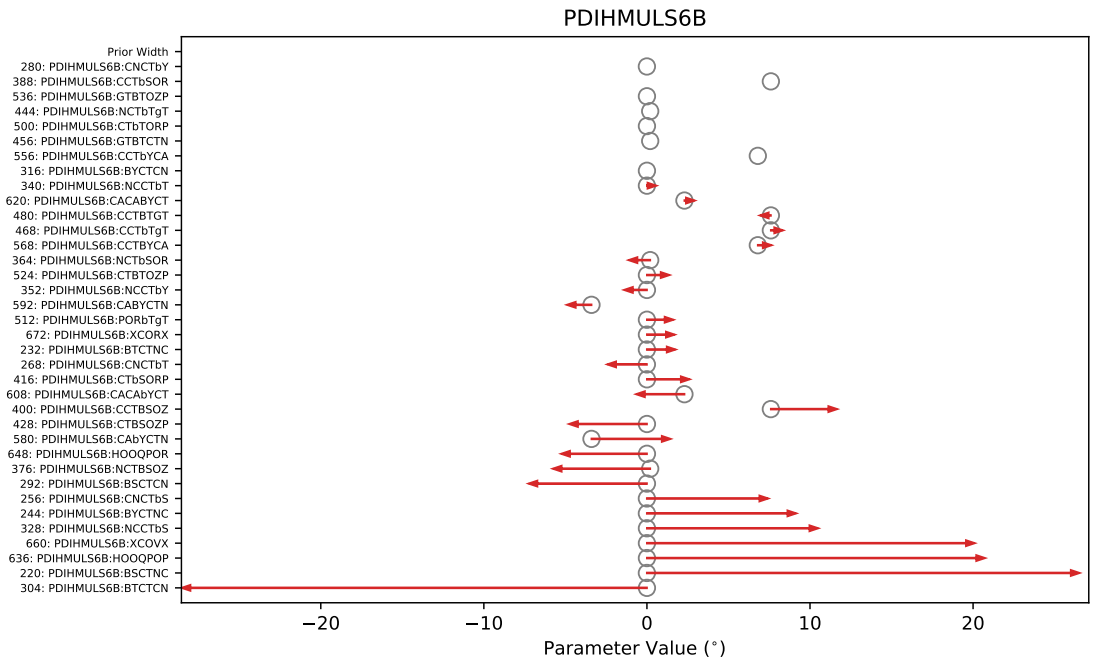

Figure S16: Parameter changes for the proper dihedral angle values (multiplicity 6).

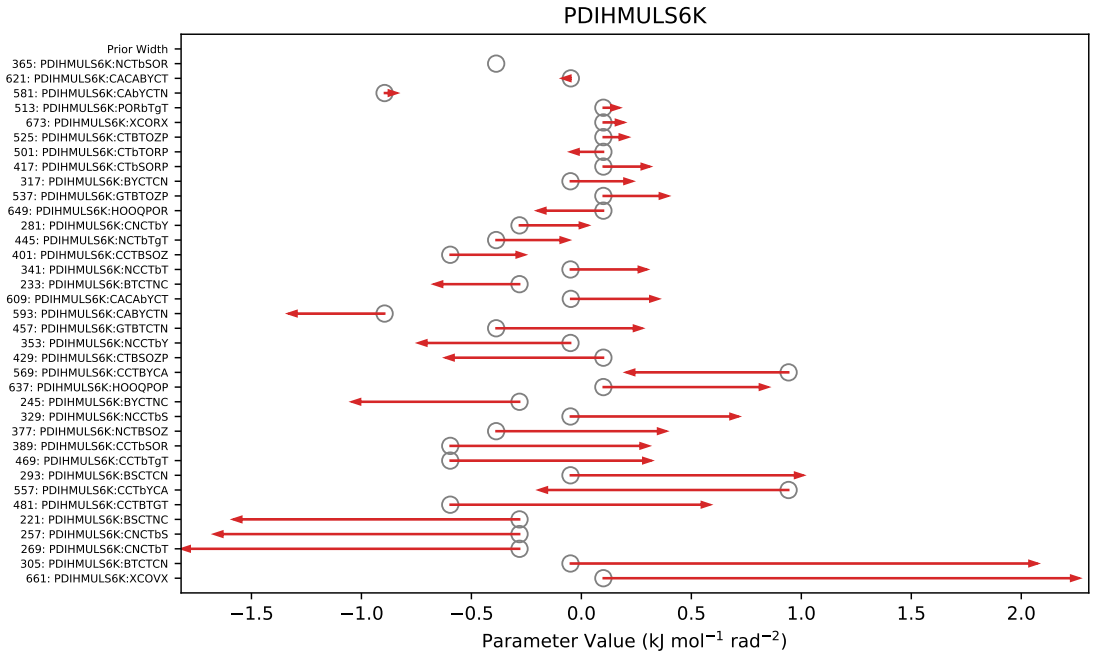

Figure S17: Parameter changes for the proper dihedral angle force constants (multiplicity 6).

1.6 Optimized Improper Dihedral Parameters

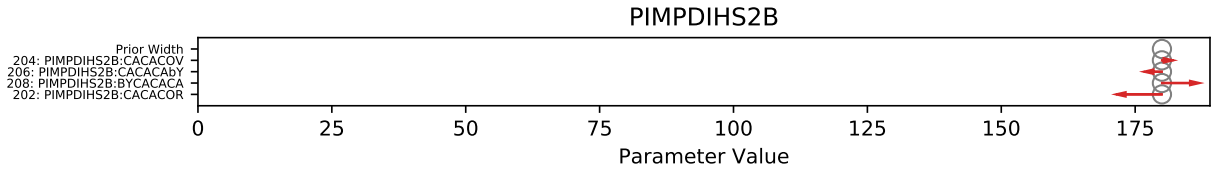

Figure S18: Parameter changes for the improper dihedral angle values.

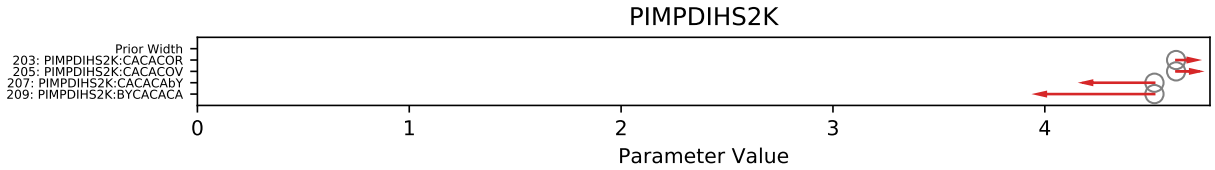

Figure S19: Parameter changes for the improper dihedral force constants.

2 Residue Heat Maps

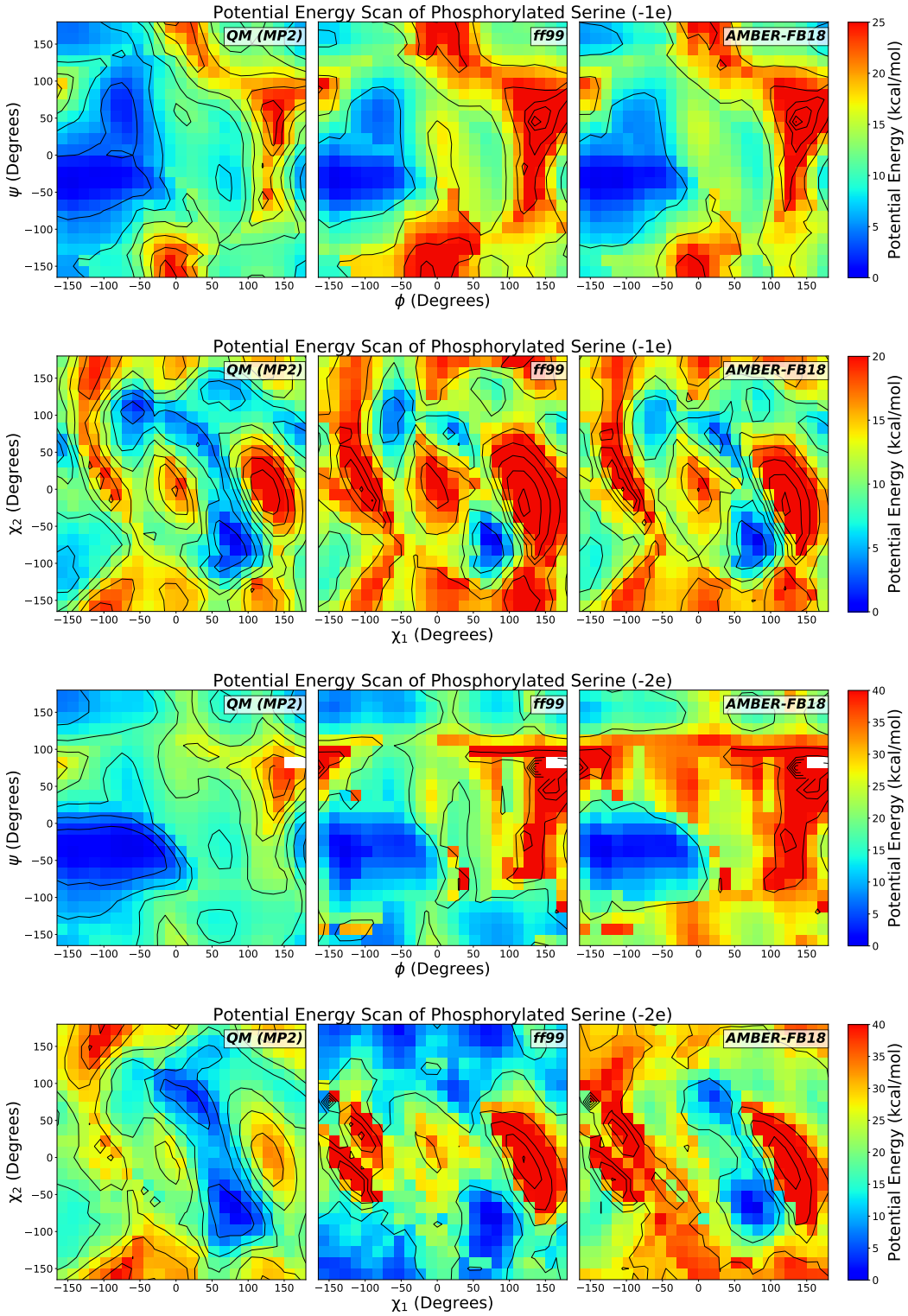

Figure S20: Heat maps for S1P and SEP, for both the (ϕ, ψ) and (χ_1, χ_2) angles

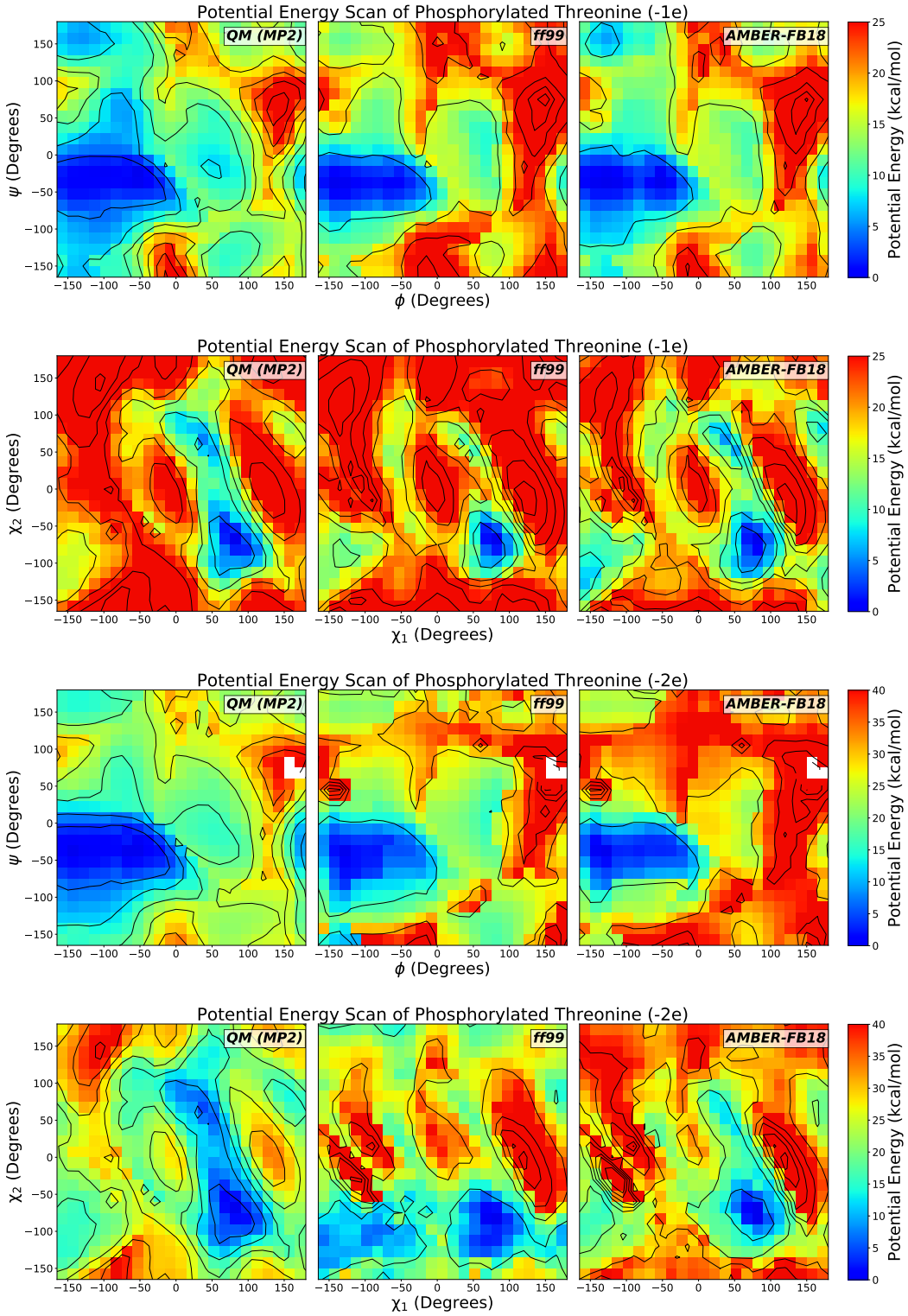

Figure S21: Heat maps for T1P and TPO, for both the (ϕ, ψ) and (χ_1, χ_2) angles

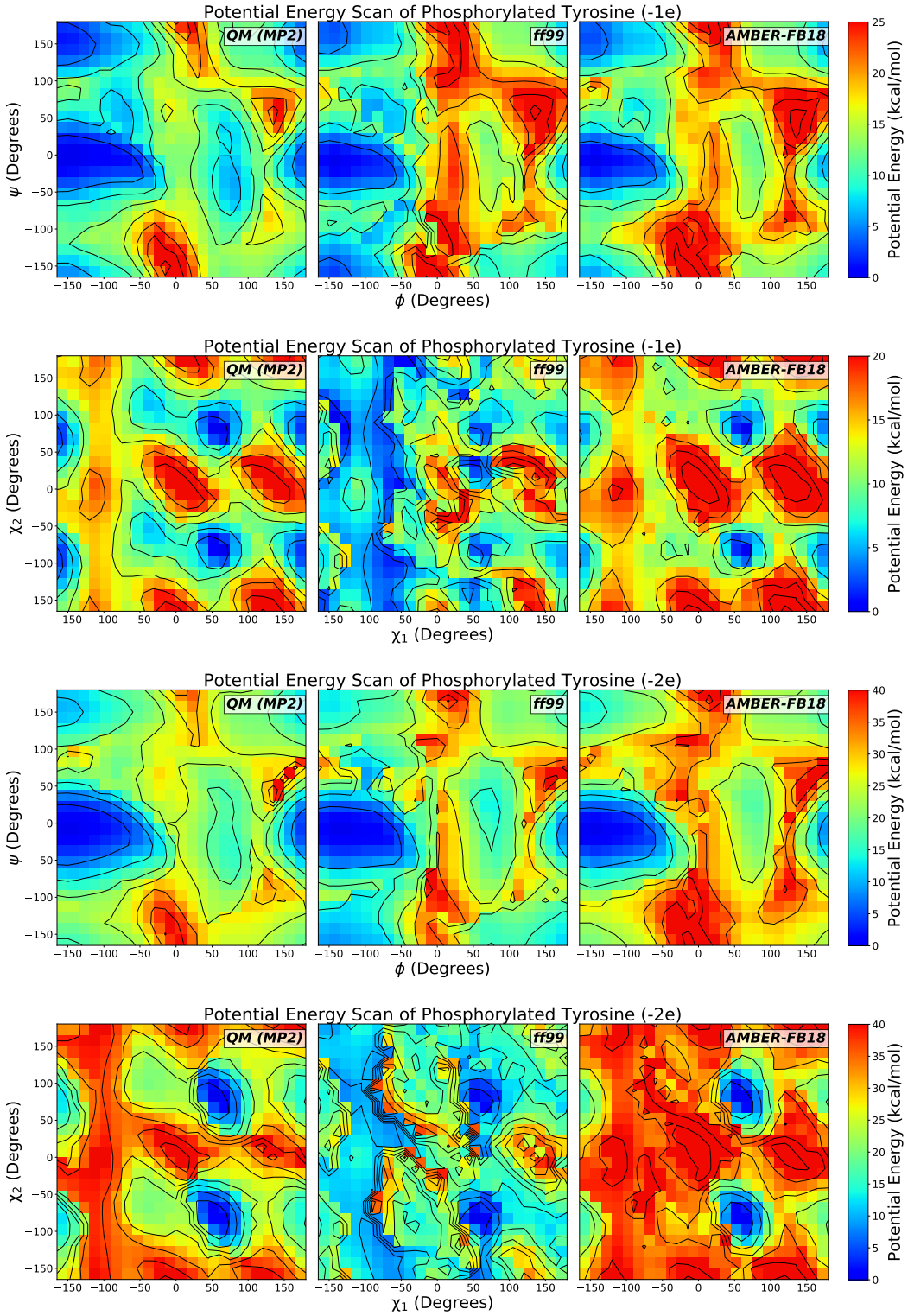

Figure S22: Heat maps for Y1P and PTR, for both the (ϕ, ψ) and (χ_1, χ_2) angles

3 Dipeptide backbone conformational preferences

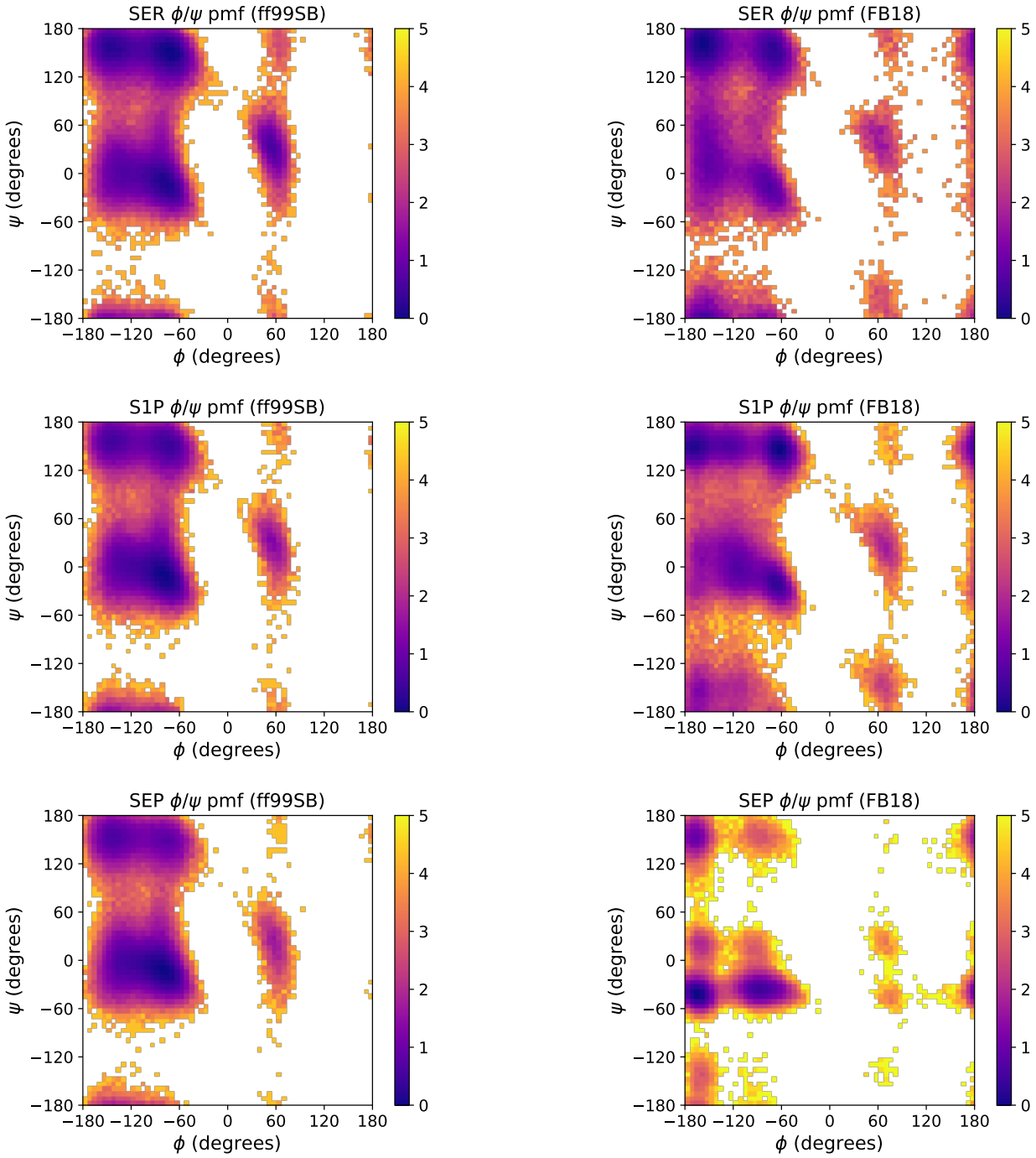

Figure S23: Potentials of mean force for ϕ/ψ backbone torsions of SER, S1P, and SEP: results obtained with ff99SB (left) and FB18 (right). Relative free energies are given in kcal/mol.

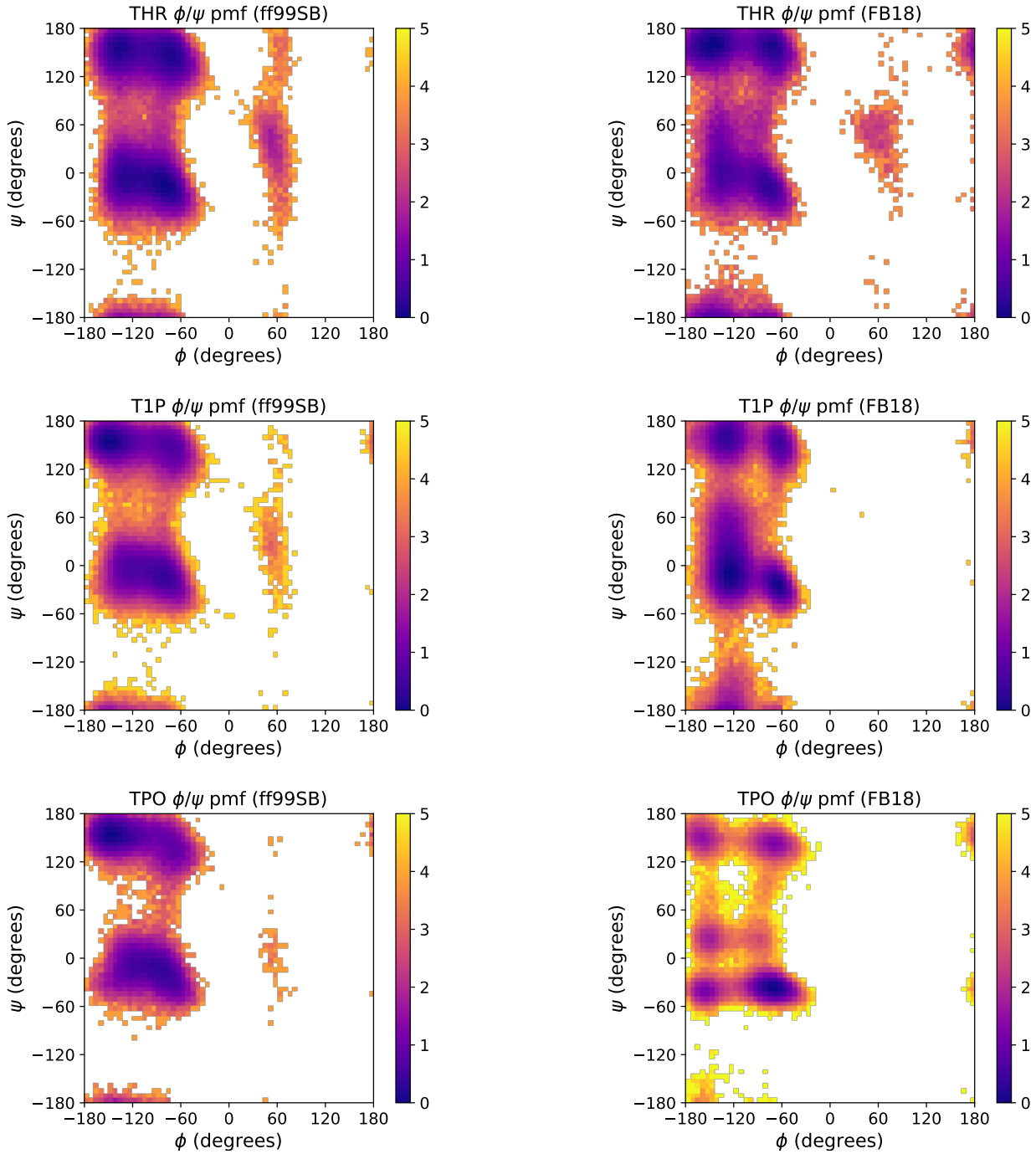

Figure S24: Potentials of mean force for ϕ/ψ backbone torsions of THR, T1P, and TPO: results obtained with ff99SB (left) and FB18 (right). Relative free energies are given in kcal/mol.

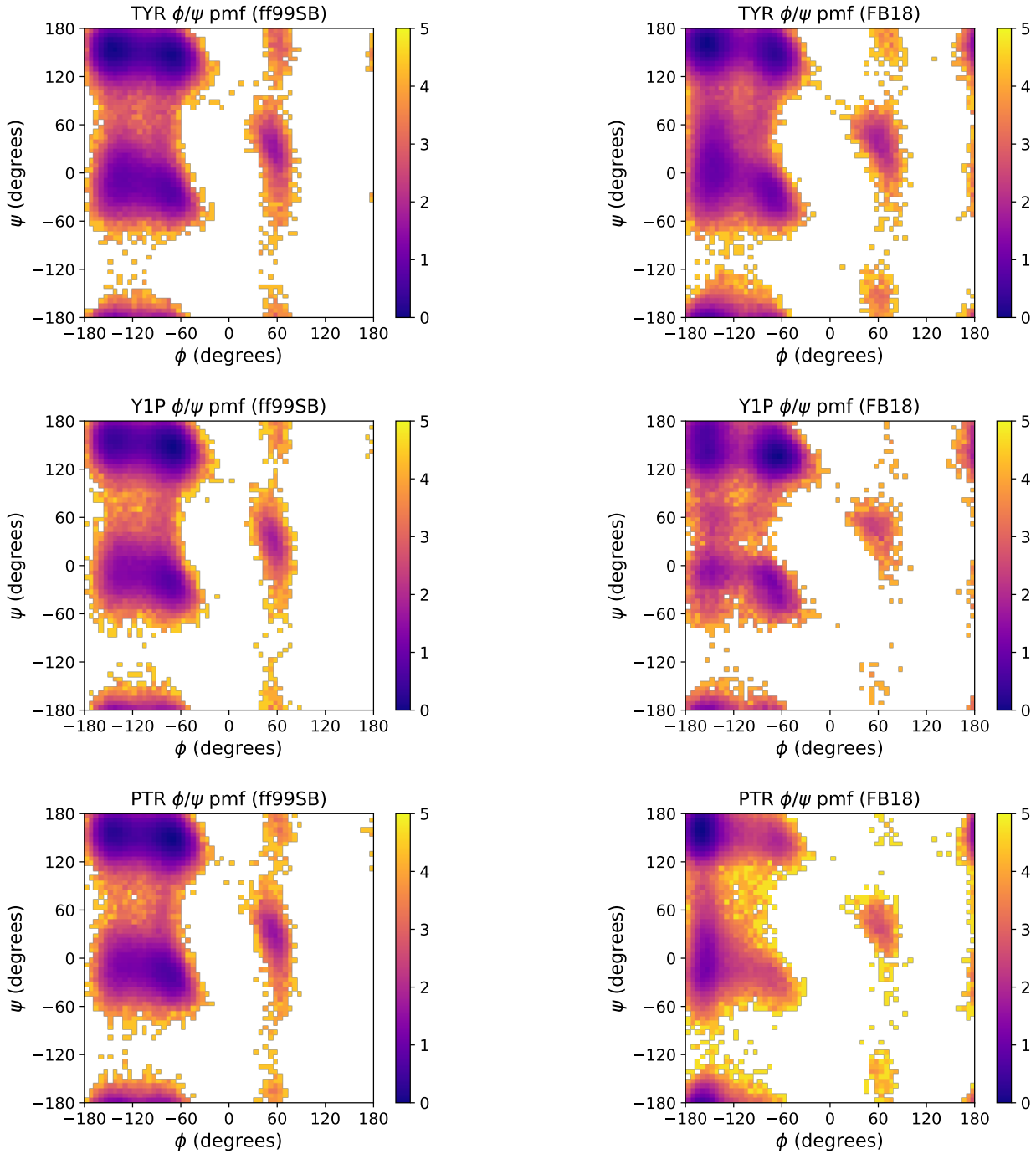

Figure S25: Potentials of mean force for ϕ/ψ backbone torsions of TYR, Y1P, and PTR: results obtained with ff99SB (left) and FB18 (right). Relative free energies are given in kcal/mol.

4 Dipeptide backbone scalar couplings

The following are backbone $^3J_{\mathrm{HN,H}\alpha}$ scalar couplings calculated using the "rigid" Karplus equation parameters given in Table 1 of Vögeli *et al.*[S3]

Table S7: Backbone $^3J_{\mathbf{HN,H}\alpha}$ Scalar Couplings (in Hz)

Residue	ff99SB	FB18	Experiment
SER	7.031 ± 0.004	6.639 ± 0.008	7.02
S1P	7.233 ± 0.011	6.309 ± 0.008	6.85
SEP	7.462 ± 0.018	6.048 ± 0.010	5.98
THR	7.511 ± 0.002	7.312 ± 0.020	7.35
T1P	7.525 ± 0.001	7.926 ± 0.004	7.55
TPO	7.576 ± 0.007	5.515 ± 0.021	5.23
TYR	7.366 ± 0.011	6.933 ± 0.001	7.13
Y1P	6.892 ± 0.012	5.851 ± 0.014	n/a
PTR	7.060 ± 0.007	6.637 ± 0.003	n/a

We then calculated the χ^2 scores for the predicted coupling data, again assuming that the σ_i^2 are dominated by the uncertainties inherent in the Karplus equation parameters themselves (in this case, RMSD: 0.42 Hz). The χ^2 scores are 6.42 and 0.57 for ff99SB and FB18, respectively. We note that these scores are significantly lower than those obtained using the "ensemble" parameters, largely because of the increase in the RMSD of the fitted Karplus equation curve for the "rigid" parameters. The overall conclusion, however, remains unchanged: FB18 is significantly more accurate than ff99SB.

References

(S1) Homeyer, N.; Horn, A. H. C.; Lanig, H.; Sticht, H. AMBER force-field parameters for phosphorylated amino acids in different protonation states: phosphoserine, phosphothreonine, phosphotyrosine, and phosphohistidine. *J. Mol. Model.* **2006**, *12*, 281–289.

(S2) Vymětal, J.; Jurásková, V.; Vondrášek, J. AMBER and CHARMM Force Fields Inconsistently Portray the Microscopic Details of Phosphorylation. *J. Chem. Theory Comput.* **2019**, *15*, 665–679.

(S3) Vögeli, B.; Ying, J.; Grishaev, A.; Bax, A. Limits on Variations in Protein Backbone Dynamics from Precise Measurements of Scalar Couplings. *J. Am. Chem. Soc.* **2007**, *129*, 9377–9385.